



# A Radiopaque Electrospun Scaffold for Engineering Fibrous Tissues: Characterization and In Vivo Application

<sup>1,2</sup>John T. Martin, MS

<sup>1,2</sup>Andrew H. Milby, MD

<sup>1</sup>Subash Poudel

<sup>1,2,3</sup>Christian G. Pfeifer, MD

<sup>1,2</sup>Harvey E. Smith, MD

<sup>4</sup>Dawn M. Elliott, PhD

<sup>1,2</sup>Robert L. Mauck, PhD

<sup>1</sup>Department of Orthopaedic Surgery,  
University of Pennsylvania,  
Philadelphia, PA, USA

<sup>2</sup>Translational Musculoskeletal Research  
Center, Philadelphia VA Medical Center,  
Philadelphia, PA, USA

<sup>3</sup>University Clinic Regensburg,  
Regensburg, Germany

<sup>4</sup>Department of Biomedical Engineering,  
University of Delaware, Newark, DE, USA

## Introduction

The healing capacity of the intervertebral disc, meniscus, tendons and ligaments is limited, and injuries to these tissues compromise function for millions.<sup>1</sup> Tissue engineering strategies for treating fibrous tissues have transitioned over the past ~15 years from *in vitro* to *in vivo* evaluation, using a variety of animal models. Once implanted, most engineered materials cannot be followed radiographically, however, and often are difficult to find at the time of sacrifice. Implant position is monitored in standard clinical practice; for example, radiopaque bone cements made of poly(methyl methacrylate) and a heavy metal salt (barium sulfate) are used in the fixation of prostheses. Enabling similar visualization of engineered soft tissues would be particularly useful for repairing tissues that are subject to physiological loads and resultant changes in position.<sup>2,3</sup> Thus, we developed a radiopaque nanofibrous scaffold by electrospinning a polymer/heavy metal salt solution, and used this material as a diagnostic tool for model development. In this study, we characterized the radiopacity, structure and mechanical behavior of the scaffold, and showed its utility in an *in vivo* model of intervertebral disc replacement.

## Methods

### Fabrication

Radiopaque scaffolds were generated from a 14.3% w/v slurry of poly( $\epsilon$ -caprolactone) (PCL) mixed with zirconium(IV) oxide (zirconia), a radiodense powder with a characteristic dimension <100 nm. Slurries were electrospun while continuously mixing, and collected onto a rotating mandrel to create an aligned nanofibrous sheet (th. = 200  $\mu$ m). Four scaffold-types with varying radiodensity were fabricated: 100% PCL, 90% PCL/10% zirconia, 75% PCL/25% zirconia, 50% PCL/50% zirconia.

### In Vitro Analysis

Each scaffold was assayed for structural continuity, radiodensity and mechanical strength. To assess nanostructure, samples were imaged by SEM (n=1/group). To measure radiodensity, 8 mm diameter samples were

punched from each scaffold and scanned by  $\mu$ CT (vivaCT 75, SCANCO) at 20  $\mu$ m resolution (n=5/group). The linear attenuation coefficient of each sample was calculated from volumetric reconstructions. Scaffold strips (5mm x 40mm) were tested in uniaxial tension in the fiber direction (n=5/group). The mechanical testing protocol consisted of a 0.05 N preload, followed by extension to failure at a rate of 0.1% strain/s. Tensile modulus was calculated as described previously.<sup>4</sup>

### In Vivo Analysis

Disc-like angle ply structures<sup>5</sup> fabricated from radiopaque scaffold (rDAPS) were implanted into the rat caudal spine.<sup>2</sup> Strips were cut from aligned radiopaque scaffold 30° to the fiber direction and two strips with alternating  $\pm$ 30° alignment were wrapped concentrically to form the annulus fibrosus region of the rDAPS. To implant rDAPS, surgical wires were passed laterally through the mid-height of vertebrae adjacent to the C8/C9 disc, and an external fixator was applied (Figure 1). A dorsal incision was made, the native disc was removed and rDAPS were inserted into the disc space. Rats were returned to cage activity and euthanized at 28 days. Two implant types were used in this study: a radiodense implant, "50/50 rDAPS" with 2 layers of 50% PCL/50% zirconia (n=2); a radiolucent implant, "75/25 rDAPS" with 1 layer of 75% PCL/25% zirconia, 1 layer 100% PCL and one layer of degradable 75:25 poly(lactic-co-glycolic acid) (PLGA, to provide a route for cell migration once degraded) (n=3). To monitor changes in implant position and structure *in vivo*, rat tails were imaged longitudinally with a fluoroscope. Then, following euthanasia, tails were imaged via  $\mu$ CT to assess implant structure and histological sections were stained with picrosirius red (for collagen).

## Results

SEM revealed that all formulations of radiopaque scaffold had continuous and aligned fibers (Figure 2A-D). Zirconia was embedded within fibers at lower concentrations, but at the highest concentration it was evident that zirconia aggregated into large pellets exterior

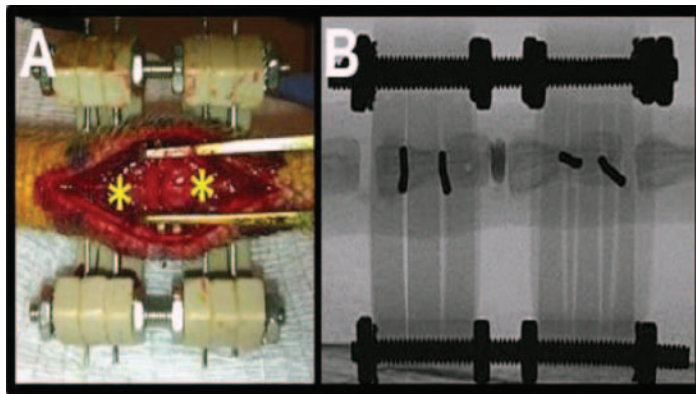


**Figure 1.** A) rDAPS were implanted between vertebrae (asterisk) of the rat caudal spine to demonstrate the utility of radiopaque scaffold. B) The vertebrae were stabilized with a radiolucent external fixator.

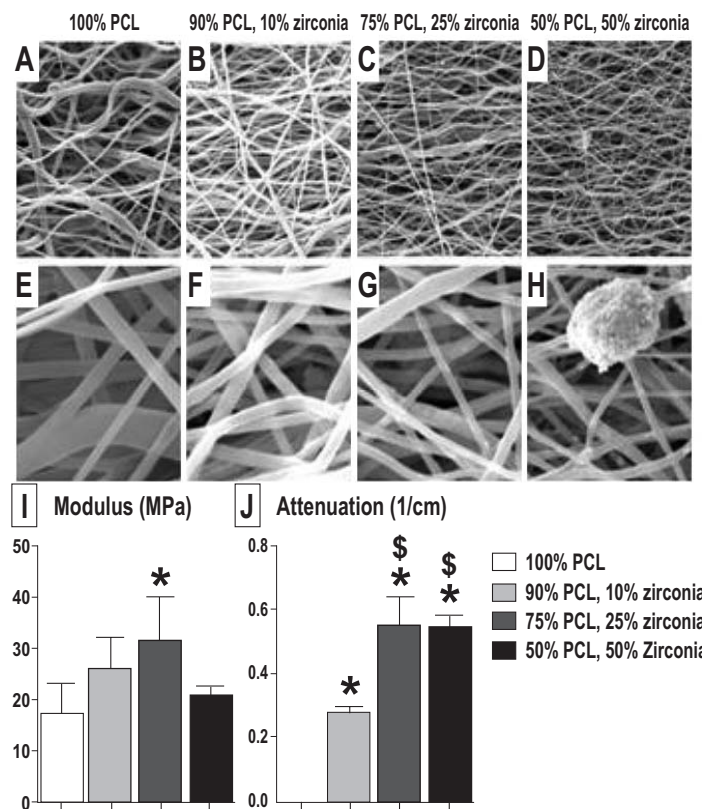


**Figure 2.** Characterization of radiopaque scaffold. SEM images at A-D) 2,000x magnification and E-H) 10,000x magnification, I) tensile modulus and J) linear attenuation. Statistics calculated using one way ANOVA with Bonferroni correction for post-hoc comparisons: \*,  $p < 0.05$  vs. 100% PCL and \$,  $p < 0.05$  from 90% PCL, 10% zirconia.

to the fibers (Figure 2E-H). In addition, as zirconia increased fiber diameter decreased. Scaffold modulus increased with zirconia content, except at the highest concentration (Figure 2I). Scaffold radiation attenuation increased with zirconia content plateauing at 25% zirconia (Figure 2J). PCL alone had no signal and thus 3D reconstruction was not possible. Both formulations of rDAPS were visualized intra- and post-operatively. 50/50 rDAPS had a distinct signal (Figure 3A), more intense than that of the native bone, while the 75/25 rDAPS

cast a radiolucent shadow similar to bone (Figure 4A). rDAPS remained in the disc space over 28 days with no change in position or shape. These results were confirmed by  $\mu$ CT; both types of rDAPS had a signal distinguishable from bone allowing for the reconstruction of each separately. Reconstructions of 50/50 rDAPS demonstrated that the radiopaque implants occupied the disc space and did not cause an adverse reaction (Figure 3B). 3D reconstructions of 75/25 rDAPS demonstrated that lamellar structure was intact after 28 days (Figure 4B,C). Images of histological sections confirmed that new collagen was deposited between layers, though the PLGA had not completely degraded (Figure 4D).

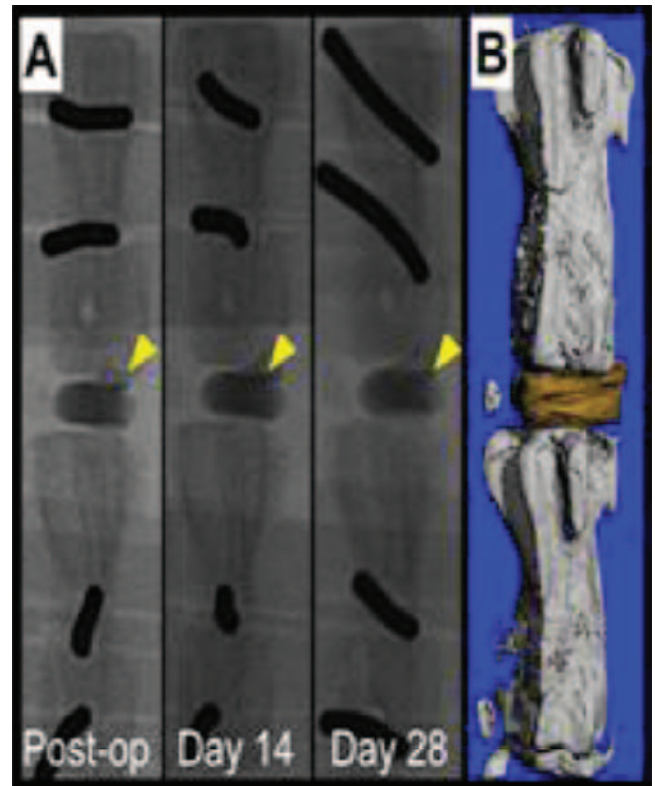


**Figure 3.** Implantation of high radiodensity rDAPS. A) Fluoroscopy over 28 days. B)  $\mu$ CT reconstruction after 28 days.

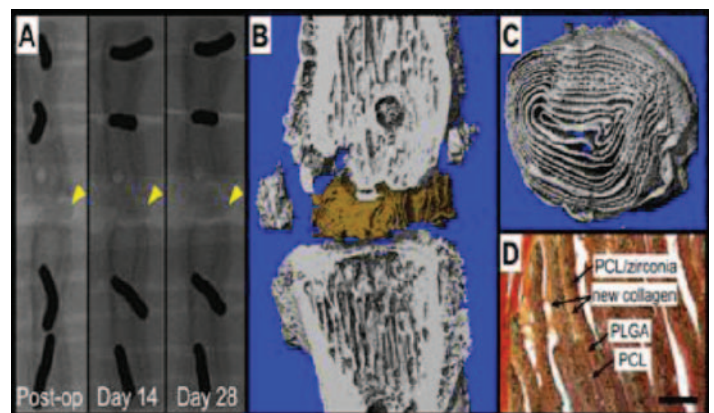


**Figure 4.** Implantation of low radiodensity rDAPS. A) Fluoroscopy over 28 days. B)  $\mu$ CT at day 28. C)  $\mu$ CT of rDAPS only at day 28. D) Picrosirius red-stained section at day 28. Scale = 250 $\mu$ m.

## Discussion

We developed and characterized a radiopaque electrospun scaffold composed of PCL, a standard tissue engineering polymer, and zirconia, a heavy metal salt. We demonstrated that scaffold radiopacity and mechanics can be tuned by altering the concentration of zirconia. In addition, we fabricated radiopaque implants and validated a rat caudal spine model of disc replacement.

Scaffold mechanical properties and radiation attenuation are tunable by altering zirconia concentration. Mechanical properties increased by adding the radiopaque filler, but declined at the highest concentration. This phenomenon is also observed in electrospun scaffolds mixed with hydroxyapatite for bone tissue engineering.<sup>6</sup> The radiation attenuation of each scaffold increased with zirconia content and plateaued at 25% zirconia. By controlling the zirconia content, scaffold radiopacity can be tuned for a specific application. For example, in a subcutaneous model, a radiolucent scaffold may be useful, since the superficial nature of a subcutaneous model lends itself to unobstructed visualization. However, if an electrospun scaffold is used to regenerate a deeper tissue, like inside a synovial joint,<sup>7</sup> the abdomen,<sup>8</sup> or within the lumbar spine, model development may require a radiodense scaffold.

Radiopaque implants made with high and low concentrations of zirconia were visualized in the rat caudal spine. Previous work with this model demonstrated that implants were ejected from the disc space when the rat tail was not fixed.<sup>2</sup> Thus, this study demonstrates that fixation is necessary for rat caudal disc replacement. In addition, the radiopaque scaffold was compatible with the formation of new collagen by endogenous cells. Future work must confirm

that these scaffolds do not influence cells to also produce mineralized tissue.

## Significance

This study describes a radiopaque scaffold for engineering fibrous tissues and its application when fluoroscopy is useful for evaluation of the scaffold in an animal model.

## Acknowledgments

Funded by the DOD

## References

1. Parenteau N, Hardin-Young J, Shannon W, et al. Meeting the need for regenerative therapies I: target-based incidence and its relationship to U.S. spending, productivity, and innovation. *Tissue Eng. Part B Rev.* 18, 139–154 (2012).
2. Martin. TORS 2013.
3. Bowles RD, et al. Image-based tissue engineering of a total intervertebral disc implant for restoration of function to the rat lumbar spine. *NMR Biomed.* 25, 443–451 (2012).
4. Baker BM, Nerurkar NL, Burdick JA, et al. Fabrication and modeling of dynamic multipolymer nanofibrous scaffolds. *J. Biomech. Eng.* 131, 101012 (2009).
5. Nerurkar N L, Sen S, Huang AH, et al. Engineered disc-like angle-ply structures for intervertebral disc replacement. *Spine* 35, 867–873 (2010).
6. Venugopal J, Low S, Choon AT, et al. Electrospun-modified nanofibrous scaffolds for the mineralization of osteoblast cells. *J Biomed Mater Res A* 85:408-17 (2008).
7. Chainani A et al. Multilayered electrospun scaffolds for tendon tissue engineering. *Tissue Eng. Part A* 19, 2594–2604 (2013).
8. Hong Y, Takanari K, Amoroso NJ, et al. An elastomeric patch electrospun from a blended solution of dermal extracellular matrix and biodegradable polyurethane for rat abdominal wall repair. *Tissue Eng Part C Methods*, 18:122-32 (2012).